

HEAD AND NECK



MRI radiomics may predict early tumor recurrence in patients with sinonasal squamous cell carcinoma

Chae Jung Park^{1†}, Seo Hee Choi^{2†}, Dain Kim³, Si Been Kim⁴, Kyunghwa Han⁵, Sung Soo Ahn⁵, Won Hee Lee², Eun Chang Choi⁶, Ki Chang Keum^{2†} and Jinna Kim^{5*†} 

Abstract

Objectives Sinonasal squamous cell carcinoma (SCC) follows a poor prognosis with high tendency for local recurrence. We aimed to evaluate whether MRI radiomics can predict early local failure in sinonasal SCC.

Methods Sixty-eight consecutive patients with node-negative sinonasal SCC (January 2005–December 2020) were enrolled, allocated to the training ($n = 47$) and test sets ($n = 21$). Early local failure, which occurred within 12 months of completion of initial treatment, was the primary endpoint. For clinical features (age, location, treatment modality, and clinical T stage), binary logistic regression analysis was performed. For 186 extracted radiomic features, different feature selections and classifiers were combined to create two prediction models: (1) a pure radiomics model; and (2) a combined model with clinical features and radiomics. The areas under the receiver operating characteristic curves (AUCs) were calculated and compared using DeLong's method.

Results Early local failure occurred in 38.3% (18/47) and 23.8% (5/21) in the training and test sets, respectively. We identified several radiomic features which were strongly associated with early local failure. In the test set, both the best-performing radiomics model and the combined model (clinical + radiomic features) yielded higher AUCs compared to the clinical model (AUC, 0.838 vs. 0.438, $p = 0.020$; 0.850 vs. 0.438, $p = 0.016$, respectively). The performances of the best-performing radiomics model and the combined model did not differ significantly (AUC, 0.838 vs. 0.850, $p = 0.904$).

Conclusion MRI radiomics integrated with a machine learning classifier may predict early local failure in patients with sinonasal SCC.

Clinical relevance statement MRI radiomics intergrated with machine learning classifiers may predict early local failure in sinonasal squamous cell carcinomas more accurately than the clinical model.

Key Points

- A subset of radiomic features which showed significant association with early local failure in patients with sinonasal squamous cell carcinomas was identified.

[†]Chae Jung Park and Seo Hee Choi contributed equally to this paper as co-first authors.

[†]Ki Chang Keum and Jinna Kim contributed equally to this paper as co-senior authors.

*Correspondence:

Jinna Kim
jinna@yuhs.ac

Full list of author information is available at the end of the article

- MRI radiomics integrated with machine learning classifiers can predict early local failure with high accuracy, which was validated in the test set (area under the curve = 0.838).
- The combined clinical and radiomics model yielded superior performance for early local failure prediction compared to that of the radiomics (area under the curve 0.850 vs. 0.838 in the test set), without a statistically significant difference.

Keywords Squamous cell carcinoma, Prognosis, Magnetic resonance imaging, Radiomics

Introduction

Sinonasal malignancies are relatively rare but aggressive tumors, accounting for 3–5% of all head and neck cancers [1]. The majority of sinonasal malignancies are epithelial neoplasms, with squamous cell carcinomas (SCCs) being the most common type accounting for approximately 38% [2]. Despite the continued emergence of new treatment options such as chemotherapy and radiotherapy, the 5-year overall survival rates were reported to remain at 20–57% [3–6]. Moreover, most patients tend to be in an advanced stage of the disease at initial presentation, because sinonasal malignancies tend to be asymptomatic or have non-specific sinonasal symptoms, until they invade adjacent structures.

Surgical resection is preferentially indicated for all operable sinonasal SCCs, although no randomized trials have been conducted to devise the optimal treatment strategy for sinonasal tumors because of their rarity and heterogeneity. Adjuvant radiotherapy (RT) is also indicated in patients with advanced-stage disease and/or high-risk features [7, 8]. However, local failure is the principal cause (approximately 50%) of relapse [8–11], since local invasion generally occurs early in the natural history of sinonasal cancers and resection is often limited by tumor involvement that can result in damage to adjacent critical structures. Intensified local therapies such as advanced surgical techniques, radiation dose escalation, and modern RT techniques have been investigated vigorously [10, 12–14]. Therefore, it is highly desirable to identify patients at high risk for local failure at the time of diagnosis, since they could be provided with more intensified treatment regimens. Furthermore, patients at low risk for local failure can be saved from aggressive intensified treatment to avoid unnecessary treatment-related complications.

Radiomics extracts high-dimensional quantitative imaging features (such as intensity distributions, spatial relationships, textural heterogeneity, and shape descriptors); thus, hidden invisible information based on imaging can be identified using radiomics studies [15, 16]. Radiomics has potential as it can reflect intra-tumoral heterogeneity using a variety of mathematical methods used to quantify gray-level spatial variations within an image to derive textural features [17]. Therefore, radiomics has also been used in the field of head and neck

cancers to predict specific molecular markers, recurrence, treatment responses, or survival [18]. As for the sinonasal tumors, MRI radiomics has proved its values for distinguishing SCC from lymphoma [19] or differentiating between benign or malignant tumors [20, 21]. However, whether radiomics also has prognostic potential to predict patient outcome in patients with sinonasal SCCs has not been well established.

In this study, we postulated that the application of radiomics to pretreatment MRI may enable prediction of early local failure in patients with sinonasal SCC. Therefore, this study aimed to evaluate whether MRI radiomics can predict early local failure in patients with sinonasal SCC to allow opportunities for more intensified local treatments in this population.

Materials and methods

Patients

This retrospective study was approved by the Institutional Review Board of our tertiary academic institution (9-2021-0111), which waived the requirement for obtaining informed patient consent. A total of 137 patients newly diagnosed with node-negative sinonasal SCC at OOO between January 2005 and December 2020 were identified. Given the purpose of the study, we excluded node-positive cases at diagnosis in order to construct a homogenous cohort. The exclusion criteria were as follows: (1) loss to follow-up during the 12-month period after initial diagnosis ($n = 48$); (2) unavailability of either T2-weighted (T2) or post-contrast T1-weighted (T1C) images ($n = 11$), and (3) inadequate image quality ($n = 10$). Finally, 68 patients who received some form of curative-intent treatment with a sufficient follow-up period (> 12 months) at our institution and eligible pretreatment MRIs were enrolled.

Patients who underwent MRI before January 2017 were allocated to the training set ($n = 47$), and those who underwent MRI after January 2017 were allocated to the test set ($n = 21$), to perform temporal validation.

Data collection and outcome definitions

The patients' age and type of treatment were retrieved from the electronic medical records. The different types of initial treatment were as follows: (1) neoadjuvant RT followed by surgical resection; (2) surgical resection only;

(3) surgical resection followed by adjuvant RT; and (4) definitive RT with or without chemotherapy. Postoperative RT was also performed for those at a high risk of local recurrence (e.g., advanced T stage, positive margins, perineural invasion, and lymphovascular invasion). The location of the tumor was also recorded, which included the maxillary sinus, nasal cavity, ethmoid sinus, sphenoid sinus, or frontal sinus. If the tumor involved multiple paranasal sinuses, the epicenter of the tumor was regarded as the tumor location. Two dedicated head and neck radiologists (C.J.P. and J.K., with 5 and 16 years of experience, respectively) independently assessed the clinical stage of the sinonasal SCCs using the pretreatment MRI according to the 8th American Joint Committee on Cancer TNM system [22], and the consensus was reached in the event of disagreement.

We also reviewed the pattern of initial treatment failure and time to relapse for the study population. The primary endpoint of our study was an early local failure, which occurred within 12 months after response to initial curative treatment. Local failure was defined as any failure occurring in structures located in proximity to the primary tumor site, either isolated or concomitant with regional or distant failures.

Image acquisition

All patients underwent MRI with a 3-T system (InteraAchieva or Achieva TX; Philips Medical Systems) and head and neck coil. The detailed MRI parameters are presented in Supplementary material S1.

Image preprocessing and radiomic feature extraction

First, the T2 and T1C images were resampled to an identical spatial resolution of $1 \times 1 \times 1$ mm using Nilearn (<https://nilearn.github.io>). Second, these images were subjected to N4 bias correction to eliminate low-frequency intensity and non-uniformity [23, 24]. Finally, the T2 images were registered to identical spatial coordinates with T1C as a template using SimpleITK (<http://www.simpleitk.org>). The signal intensity was normalized using the WhiteStripe R package [25] which is implemented in R software (version 3.5.1, R Foundation for Statistical Computing; www.R-project.org). The ROIs were drawn by two dedicated head and neck radiologists (C.J.P. and J.K., with 5 and 16 years of experience, respectively) and the inter-rater radiomic feature stability was calculated using the intraclass correlation coefficient (ICC). As all the tumors showed variable degrees of contrast enhancement, the tumors were well visualized on 3D T1C images. The hemorrhagic and necrotic areas of the tumor were also included in the ROI. The segmentation was performed with a semiautomatic method of signal intensity threshold using the Medical Image Processing,

Analysis, and Visualization software version 7.0 (National Institutes of Health; mipav.cit.nih.gov).

The radiomic features were extracted from the ROIs drawn on the T2 and T1C images using Pyradiomics 2.0 (<http://www.radiomics.io/pyradiomics.html>) [26]. The detailed pipelines for image preprocessing and radiomic feature extraction are presented in Fig. 1.

Fourteen shapes, 18 first-orders, 24 gray-level co-occurrence matrices (GLCM), 16 gray-level run-length matrices (GLRLM), 16 gray-level size zone matrices (GLSZM), and 5 neighborhood gray-tone difference matrices (NGTDM) were extracted from the ROIs drawn on the T2 and T1C images, constituting a total of 186 radiomic features.

Feature selection and classification methods

Feature selection and classification were performed using the R software (version 3.5.1). To avoid collinearity and minimize the potential risk of overfitting while handling high-dimensional radiomic features [27, 28], the least absolute shrinkage and selection operator (LASSO) and recursive feature elimination (RFE) were used to select the important features using the “caret” R package [29]. Feature selection was performed before model construction using either LASSO, RFE, or RFE + LASSO, where LASSO was performed after RFE to further minimize the redundant features. Three subsets of selected features were combined with four different machine learning classifiers: XGboost, support vector machine (SVM), linear discriminant analysis (LDA), and adaptive boosting (AdaBoost). For each classifier, a grid search method was performed in which the hyperparameters with the highest area under the curve (AUC) by using the three times repeated 5-fold cross-validation were determined. The detailed hyperparameter settings of classifiers are presented in Supplementary material S2.

Statistical analysis

Statistical analysis was performed using the R software (version 3.5.1). Two-sided p values < 0.05 were considered to indicate statistically significant differences.

The inter-observer variability of radiomic features was studied using the ICC [30], based on the two-way mixed effects model with consistency assumption [31]. We considered a feature is reproducible if $ICC \geq 0.8$, based on previous studies which adopted 0.8 as a threshold [32]. Only reproducible radiomic features with $ICC \geq 0.8$ were included in the subsequent analysis.

Random oversampling examples were adopted to resolve the imbalance in the training set [33]. Better classifier performance than that yielded by only undersampling of the majority class was achieved by a

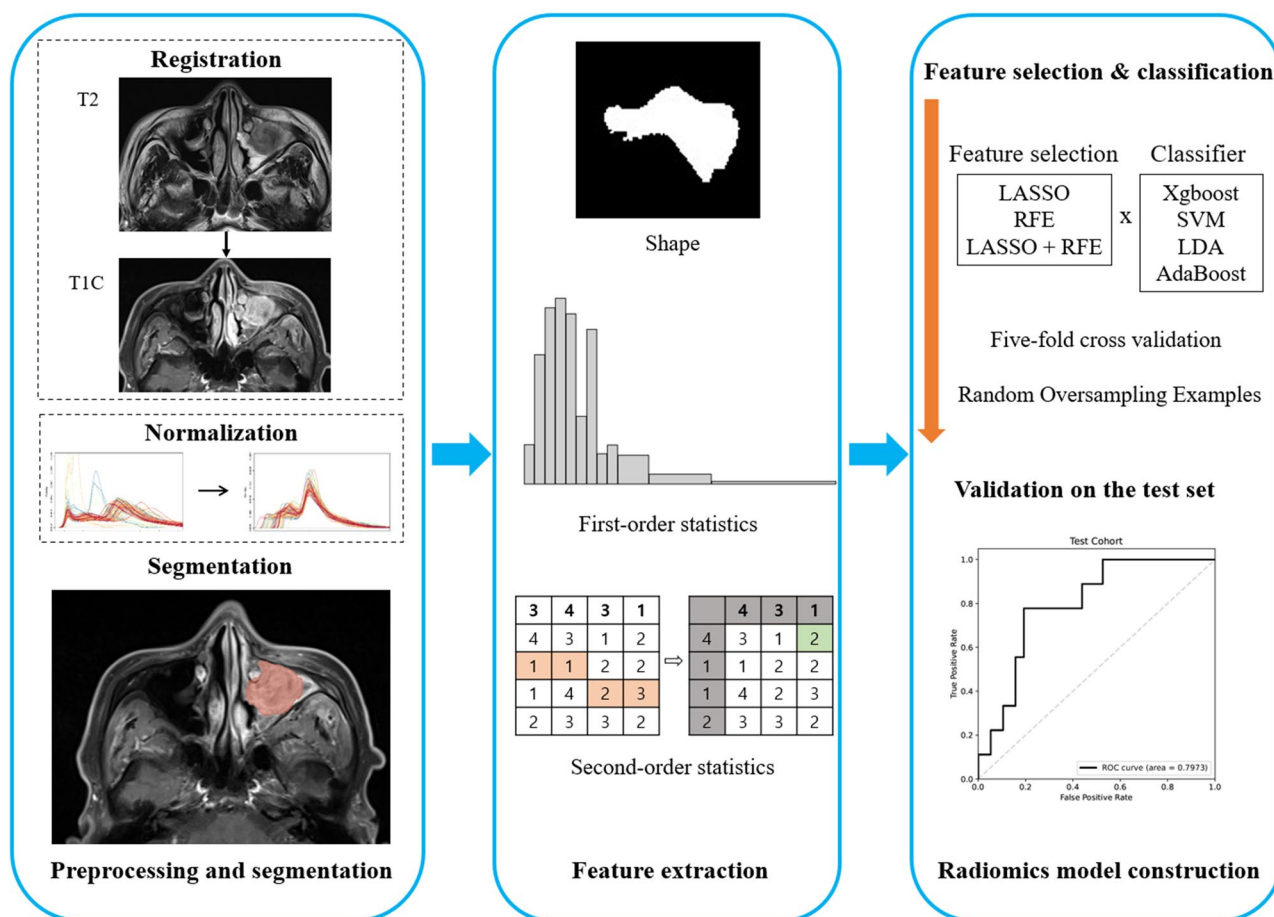


Fig. 1 Workflow of image preprocessing, radiomics feature extraction, and machine learning

combination of oversampling of the minority class and undersampling of the majority class.

We built two different models using radiomics which were developed in the training set: (1) model 1 with radiomic features only; and (2) model 2 with both clinical (age, tumor location, type of treatment, and clinical T stage) and radiomic features. Twelve combinations of the above-mentioned feature selection methods and machine learning classifiers were used for the development of models 1 and 2. These models were validated in the test set. In addition, binary logistic regression analysis was performed to develop a clinical model including age, tumor location, type of treatment, and clinical T stage. Receiver operating characteristic curves were obtained and the area under the receiver operating characteristic curves (AUC) was calculated to measure the predictive performance. The AUCs of different models were compared using Delong’s method and multiple comparisons were corrected using the Benjamini-Hochberg procedure [34].

Results

The baseline characteristics of 68 patients are presented in Table 1. The age, sex, tumor location, treatment type, and clinical T stage did not differ significantly between the training and test sets. Forty-six patients underwent surgery first (with additional adjuvant RT for 44 patients), 3 patients underwent surgery after neoadjuvant RT, and 19 patients received RT as primary treatment without surgery due to tumor unresectability and medical unsuitability. Forty-five patients (68.2%) underwent chemotherapy alone or in combination with RT.

The median follow-up duration was 32.5 months (range, 12–167.3). There were 38 instances of failure (55.9%) after the first primary treatments, of which 35 occurred within 12 months after completion of the initial curative treatment (defined as “early failure”). Among them, 23 patients had early local failure; 17 patients only had local failure, while the remaining 6 patients had both local and regional/distant metastases. Eighteen (18/47, 38.3%) and 5 (5/21, 23.8%) patients

Table 1 Patients' clinical characteristics

		Training set (n = 47)	Test set (n = 21)	p value ^a
Age (years)		56.0 (49.0–64.5)	61.0 (57.0–67.0)	0.172
Sex	Male	38	14	0.334
	Female	9	7	
Tumor location	Maxillary sinus	37 (78.7%)	17 (81.0%)	0.833
	Ethmoid sinus and nasal cavity	8 (17.0%)	4 (19.0%)	
	Sphenoid sinus	2 (4.3%)	0 (0.0%)	
Clinical T stage	T2	4 (8.5%)	3 (14.3%)	0.220
	T3	24 (51.1%)	6 (28.6%)	
	T4	19 (40.4%)	12 (57.1%)	
Treatment	Neoadjuvant RT (± CTx) + surgery	1 (2.1%)	2 (9.5%)	0.643
	Surgery only	1 (2.1%)	1 (4.8%)	
	Surgery + adjuvant RT (± CTx)	30 (63.8%)	14 (66.7%)	
	Definitive RT (± CTx)	15 (31.9%)	4 (19.0%)	

Data are expressed as medians with interquartile range in parentheses, or number of patients with the percentage in parentheses

RT radiotherapy, CTx chemotherapy

^a Comparisons between the training set and the test set using the Student *t*-test for continuous variables and chi-squared test for categorical variables

from the training and test sets, respectively, experienced early local failure.

The mean ICC of radiomic features was 0.950, and of the radiomic features with ICC \geq fea was 178/186 (95.7%). In the training set, 26, 30, and 13 features were selected through LASSO, RFE, and RFE + LASSO, respectively, which showed a significant association with early local failure. Three features, i.e., one shape feature (flatness) and three texture features (High Gray Level Zone Emphasis, Cluster Prominence, and coarseness from T2 images), were consistently selected in all three methods.

All the AUCs of model 1 (radiomic features only) with different combinations of feature selection methods and classifiers for the training and test sets, respectively, are

presented in Fig. 2. The confidence interval for each AUC is presented in Supplementary material S3. In the training set, model 1 accurately predicted early local failure in sinonasal SCC with high AUCs, ranging from 0.901 to 1. In the test set, the AUCs of model 1 ranged from 0.369 to 0.838. The combination of LDA with RFE showed the highest predictive performance with an AUC of 0.838 (95% CI, 0.615–1.000).

All the AUCs of model 2 (combination of clinical and radiomic features) with different combinations of feature selection methods and classifiers for the training and test sets, respectively, are presented in Fig. 3. The confidence interval for each AUC is presented in Supplementary material S3. In the training set, model 2 accurately

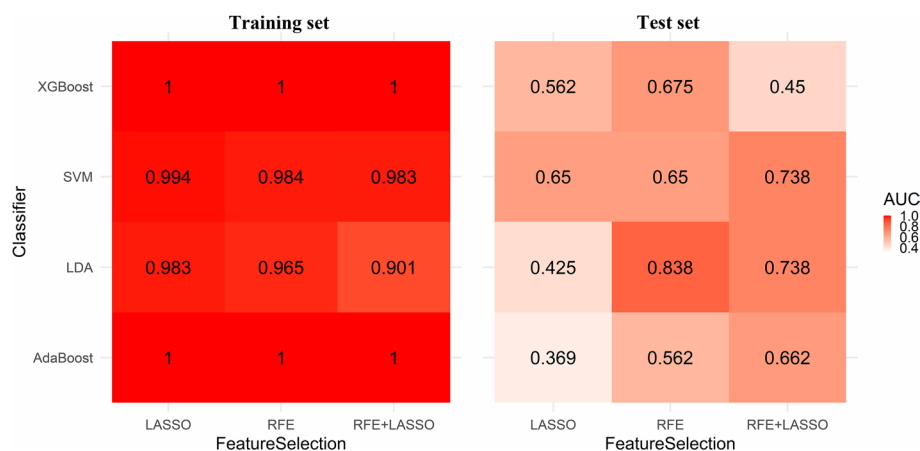


Fig. 2 Heatmaps illustrating the predictive performance (AUCs) of the different combinations of feature selection methods (rows) and classifiers (columns) from model 1 (radiomic features only) in the training and test sets. SVM support vector machine, LDA linear discriminant analysis, AdaBoost adaptive boosting, LASSO least absolute shrinkage and selection operator, RFE recursive feature elimination



Fig. 3 Heatmaps illustrating the predictive performance (AUCs) of the different combinations of feature selection methods (rows) and classifiers (columns) from model 2 (clinical and radiomics features) in the training and test sets. SVM support vector machine, LDA linear discriminant analysis, AdaBoost adaptive boosting, LASSO least absolute shrinkage and selection operator, RFE recursive feature elimination

predicted early local failure in sinonasal SCC with high AUCs, ranging from 0.919 to 1. In the test set, model 2 predicted early tumor recurrence with AUCs ranging from 0.425 to 0.850. The combination of LDA with RFE + LASSO showed the highest predictive performance with an AUC of 0.850 (95% CI, 0.623–1.000). Regarding the best-performing models, 15 different AUCs from 3 repetitions of 5-fold cross-validation are presented in Supplementary material S4.

The AUCs of the clinical model were 0.597 (95% CI, 0.467–0.727) and 0.438 (95% CI, 0.215–0.660) in the training and test sets, respectively. We compared the AUCs of the best-performing model 1 (radiomic features only) and model 2 (combination of clinical and radiomic features) to that of a clinical model in the test set. The best-performing model 1 showed significantly higher performance compared to the clinical model (AUC, 0.838 vs. 0.438, $p = 0.020$). The best-performing model 2 also showed significantly higher performance compared to the clinical model (AUC 0.850 vs. 0.438, $p = 0.016$). The performances of the best-performing model 1 and model 2 in the test set did not differ significantly ($p = 0.904$, Fig. 4).

Discussion

We identified a subset of radiomic features extracted from multiparametric MRI, which exhibited a significant association with early local failure in patients with sinonasal SCCs. By integrating radiomics with machine learning classifiers, we found that MRI radiomics can predict early local failure with high accuracy, which was validated in the test set. When the clinical features were added to radiomics, the model performance for early local failure prediction increased, albeit without a statistically significant difference. Furthermore, we showed that those

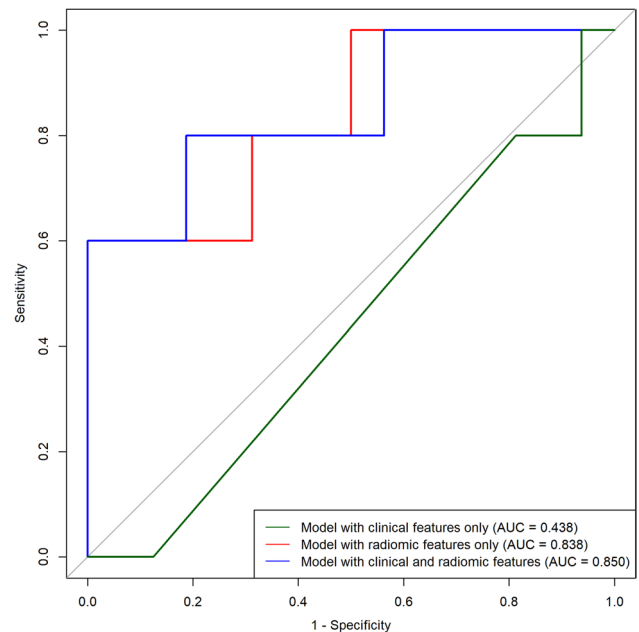


Fig. 4 Receiver operating characteristic curves of model 1 (radiomic features only) and model 2 (clinical and radiomic features) with the highest predictive performance for predicting early tumor recurrence in patients with sinonasal squamous cell carcinoma. There were no significant differences in performances between model 1 and model 2 ($p = 0.904$)

radiomics model either with or without clinical features achieved superior performances compared to the clinical model with statistical significances. Therefore, our results suggest that MRI radiomics may be used as a potential imaging biomarker in patients with sinonasal SCCs.

Many studies have recently adopted radiomics in the field of head and neck cancer as well as common solid tumor research, in order to predict specific molecular

markers, locoregional recurrence, treatment response, or survival, as radiomics is a novel quantitative imaging analysis method that utilizes high-dimensional, mineable features via high-throughput extraction, revealing the predictive and prognostic role of radiomics. CT radiomic features have been used more frequently compared to MRI, although MRI radiomics are also employed, especially in patients with nasopharyngeal and oropharyngeal cancers [18, 35]. The potential of MRI radiomics in distinguishing between SCC and lymphoma [19] or to differentiate between benign or malignant tumors has been validated in patients with sinonasal tumors [20, 21]. However, little is known about the prognostic role of radiomics in patients with SCCs arising from the sinonasal cavity. Therefore, in our study, we applied radiomics to conventional T2 and T1C imaging, which are the key sequences for tumor characterization, and concluded that multiparametric MRI radiomics can predict early tumor recurrence with high accuracy, suggesting the role of radiomics as a potential prognostic imaging biomarker.

Three texture features—High Gray Level Zone Emphasis, Cluster Prominence, and coarseness, acquired from T2-weighted images—were found to have a significant association with early local failure in patients with sinonasal SCCs. High Gray Level Zone Emphasis is a GLSZM feature, which measures the distribution of the higher gray-level values: higher GLSZM values indicate a greater proportion of higher gray-level values and size zones in the image [36]. Cluster Prominence is a GLCM feature, which is a measure of the skewness and asymmetry of the GLCM. A higher value of Cluster Prominence implies greater asymmetry about the mean, while a lower value indicates a peak near the mean value and less variation about the mean [36]. Lastly, coarseness is a NGTDM feature, which is a measure of the average difference between the center voxel and its neighborhood. This is an indication of the spatial rate of change, and a higher value indicates a lower spatial change rate and a locally more uniform texture [37]. Unlike the aforementioned two selected features, coarseness had a negative correlation with early tumor recurrence, which indicates that a lower value of coarseness presenting non-uniform texture has a significant association with a worse outcome. Therefore, considering that these selected features largely reflect intra-tumoral heterogeneity, malignant sinonasal tumors with a greater degree of heterogeneity, which could be captured by selected radiomic features, may possess more aggressive tendencies with early recurrence in the follow-up period.

In our study, we applied variable combinations of commonly used machine learning classifiers and feature selection methods to yield predictive performances for both radiomics and the combined (clinical and radiomic features) models. We observed that the highest performances

in the test set derived from the combination of LDA. Even though the other classifiers, i.e., XGBoost, SVM, and AdaBoost, achieved almost perfect AUCs in the training set, the AUCs significantly decreased when validated in the test set, indicating the overfitting of those models. It is noteworthy that the LDA classifier consistently achieved high performance for outcome prediction. The superiority of the LDA classifier for the outcome prediction should be validated in future studies with larger sample sizes.

According to the current treatment guidelines [38], surgical resection is recommended first for all operable sinonasal SCCs, irrespective of nodal status. However, postoperative RT is recommended in the presence of risk factors such as perineural invasion, lymphovascular invasion, or positive surgical margins, owing to the high tendency for local recurrence and poor survival rate of sinonasal cancer. As local recurrence is the most important reason for treatment failure in patients with sinonasal SCC, accurate prediction of local recurrence may guide clinicians in formulating effective, individualized treatment regimens. Our study revealed that patients at high risk for local recurrence could be accurately identified by MRI radiomics and such a classification according to a radiomics model could be a stronger indication for enhanced postoperative treatments.

There were several limitations in our study that should be addressed. First, this study was retrospective in design and the size of the study population was small. Moreover, we were not able to perform an external validation, as an adequate number of eligible patients in the other independent institutions were not feasible. Subsequently, we validated our model using a temporal validation set in this study. Further studies with larger sample sizes and external validation sets derived from multicenter imaging data acquired using various equipment would be required for more rigorous validation. Second, we enrolled patients with node-negative sinonasal SCCs only to maintain the homogeneity of the study population because lymph node metastasis is one of the major prognostic factors in sinonasal SCCs, requiring a different treatment decision approach [3, 4, 39, 40]. As our models are limited to node-negative patients, future studies which include larger sample sizes with node-positive patients should be performed to validate our study results. Third, human papillomavirus is reported as a significant predictor of more favorable survival for sinonasal SCCs [41]; however, we were not able to analyze it as the human papillomavirus status was not available in most of the study subjects. Fourth, advanced MRI parameters, such as ADC, were not included in this study, because most participants' preoperative MRI lacked diffusion-weighted images. However, as the EPI technique is highly sensitive to susceptibility artifacts, the role of DWI is critically limited for the evaluation of sinonasal

cavity lesions due to these artifacts resulting from air in the sinonasal cavity. Further radiomic studies with advanced MRI sequences such as diffusion-weighted or perfusion-weighted imaging may enhance the prognostic role of radiomics in patients with sinonasal SCCs, if they can be acquired with acceptable imaging quality.

In conclusion, MRI radiomics integrated with a machine learning classifier may predict early tumor recurrence in patients with sinonasal SCCs, which would be of immense help in selecting patients requiring intensified local therapies.

Abbreviations

LASSO	Least absolute shrinkage and selection operator
RFE	Recursive feature elimination
RT	Radiotherapy
SCC	Squamous cell carcinoma
T2	T2-weighted image
TIC	Post-contrast T1-weighted image

Supplementary Information

The online version contains supplementary material available at <https://doi.org/10.1007/s00330-023-10389-6>.

Below is the link to the electronic supplementary material. Supplementary file 1 (PDF 254 KB)

Funding

This work was supported by a grant provided by the National Research Foundation of Korea (NRF), which is funded by the Korean Government (Ministry of Science and ICT) (No. 2019R1A2C1008409). This study was also supported by the National Research Foundation of Korea (NRF) grant funded by the Korean government (MSIT) (No. 2021R1A2C1010900) and a faculty research grant conferred by Yonsei University College of Medicine (6-2020-0115).

Declarations

Guarantor

The scientific guarantor of this publication is Jinna Kim.

Conflict of interest

The authors of this manuscript declare no relationships with any companies, whose products or services may be related to the subject matter of the article.

Statistics and biometry

One of the authors, Kyunghwa Han, is an expert in statistics in medical imaging.

Informed consent

Written informed consent was waived by the Institutional Review Board because of the retrospective nature of the study.

Ethical approval

Institutional Review Board approval was obtained (9-2021-0111).

Study subjects or cohorts overlap

The study subjects or cohorts have not been previously reported.

Methodology

- retrospective
- diagnostic or prognostic study
- performed at one institution

Author details

¹Department of Radiology, Research Institute of Radiological Science and Center for Clinical Imaging Data Science, Yonsei Severance Hospital, Yonsei University College of Medicine, Seoul, Republic of Korea. ²Department of Radiation Oncology, Yonsei Cancer Center, Heavy Ion Therapy Research Institute, Yonsei University College of Medicine, Seoul, Republic of Korea. ³Graduate School of Artificial Intelligence, Pohang University of Science and Technology, Pohang, Republic of Korea. ⁴Undergraduate School of Biomedical Engineering, Korea University College of Health Science, Seoul, Republic of Korea. ⁵Department of Radiology, Research Institute of Radiological Science and Center for Clinical Imaging Data Science, Severance Hospital, Yonsei University College of Medicine, 50-1 Yonsei-ro, Seodaemun-gu, Seoul 03722, Korea. ⁶Department of Otorhinolaryngology, Yonsei Severance Hospital, Yonsei University College of Medicine, Seoul, Republic of Korea.

Received: 15 November 2022 Revised: 28 August 2023 Accepted: 7 September 2023

Published online: 06 November 2023

References

- Dulguerov P, Jacobsen MS, Allal AS, Lehmann W, Calcaterra T (2001) Nasal and paranasal sinus carcinoma: are we making progress? A series of 220 patients and a systematic review. *Cancer* 92:3012–3029
- Youlden DR, Cramb SM, Peters S et al (2013) International comparisons of the incidence and mortality of sinonasal cancer. *Cancer Epidemiology* 37:770–779
- Cantù G, Bimbi G, Miceli R et al (2008) Lymph node metastases in malignant tumors of the paranasal sinuses: prognostic value and treatment. *Arch Otolaryngol Head Neck Surg* 134:170–177
- Bhattacharyya N (2003) Factors affecting survival in maxillary sinus cancer. *J Oral Maxillofac Surg* 61:1016–1021
- Ganly I, Patel SG, Singh B et al (2005) Craniofacial resection for malignant paranasal sinus tumors: report of an International Collaborative Study. *Head Neck* 27:575–584
- Al-Qurayshi Z, Smith R, Walsh JE (2020) Sinonasal squamous cell carcinoma presentation and outcome: a national perspective. *Annals Otol Rhinol Laryngol* 129:1049–1055
- Robbins KT, Ferlito A, Silver CE et al (2011) Contemporary management of sinonasal cancer. *Head Neck* 33:1352–1365
- Hoppe BS, Stegman LD, Zelefsky MJ et al (2007) Treatment of nasal cavity and paranasal sinus cancer with modern radiotherapy techniques in the postoperative setting—the MSKCC experience. *Int J Radiat Oncol Biol Phys* 67:691–702
- Daly ME, Chen AM, Bucci MK et al (2007) Intensity-modulated radiation therapy for malignancies of the nasal cavity and paranasal sinuses. *Int J Radiat Oncol Biol Phys* 67:151–157
- Duru Birgi S, Teo M, Dyker KE, Sen M, Prestwich RJ (2015) Definitive and adjuvant radiotherapy for sinonasal squamous cell carcinomas: a single institutional experience. *Radiat Oncol* 10:190
- Wiegner EA, Daly ME, Murphy JD et al (2012) Intensity-modulated radiotherapy for tumors of the nasal cavity and paranasal sinuses: clinical outcomes and patterns of failure. *Int J Radiat Oncol Biol Phys* 83:243–251
- Abu-Ghanem S, Horowitz G, Abergel A et al (2015) Elective neck irradiation versus observation in squamous cell carcinoma of the maxillary sinus with N0 neck: a meta-analysis and review of the literature. *Head Neck* 37:1823–1828
- Galloni C, Locatello LG, Bruno C, Cannavici A, Maggiore G, Gallo O (2021) The role of elective neck treatment in the management of sinonasal carcinomas: a systematic review of the literature and a meta-analysis. *Cancers (Basel)* 13(8):1842
- Patel SH, Wang Z, Wong WW et al (2014) Charged particle therapy versus photon therapy for paranasal sinus and nasal cavity malignant diseases: a systematic review and meta-analysis. *Lancet Oncol* 15:1027–1038
- Aerts HJWL, Velazquez ER, Leijenaar RTH et al (2014) Decoding tumour phenotype by noninvasive imaging using a quantitative radiomics approach. *Nat Comm* 5:4006
- Gillies RJ, Kinahan PE, Hricak H (2016) Radiomics: images are more than pictures, they are data. *Radiology* 278:563–577

17. Molina D, Pérez-Beteta J, Martínez-González A et al (2016) Influence of gray level and space discretization on brain tumor heterogeneity measures obtained from magnetic resonance images. *Comput Biol Med* 78:49–57
18. Haider SP, Burtress B, Yarbrough WG, Payabvash S (2020) Applications of radiomics in precision diagnosis, prognostication and treatment planning of head and neck squamous cell carcinomas. *Cancers Head Neck* 5:6
19. Wang X, Dai S, Wang Q, Chai X, Xian J (2021) Investigation of MRI-based radiomics model in differentiation between sinonasal primary lymphomas and squamous cell carcinomas. *Jpn J Radiol* 39:755–762
20. Bi SC, Zhang H, Wang HX et al (2021) Radiomics nomograms based on multi-parametric MRI for preoperative differential diagnosis of malignant and benign sinonasal tumors: a two-centre study. *Front Oncol* 11:659905
21. Zhang H, Wang H, Hao D et al (2021) An MRI-based radiomic nomogram for discrimination between malignant and benign sinonasal tumors. *J Magn Reson Imaging* 53:141–151
22. Amin MBES, Greene F, Byrd DR, Brookland RK, Washington MK, Gershenwald JE, Compton CC, Hess KR et al (2017) *AJCC cancer staging manual*, 8th edn. American Joint Commission on Cancer, Springer International Publishing
23. Tustison NJ, Avants BB, Cook PA et al (2010) N4ITK: improved N3 bias correction. *IEEE Trans Med Imaging* 29:1310–1320
24. Sled JG, Zijdenbos AP, Evans AC (1998) A nonparametric method for automatic correction of intensity nonuniformity in MRI data. *IEEE Trans Med Imaging* 17:87–97
25. Shinohara RT, Sweeney EM, Goldsmith J et al (2014) Statistical normalization techniques for magnetic resonance imaging. *Neuroimage Clin* 6:9–19
26. van Griethuysen JJM, Fedorov A, Parmar C et al (2017) Computational radiomics system to decode the radiographic phenotype. *Cancer Res* 77:e104–e107
27. Friedman J, Hastie T, Tibshirani R (2010) Regularization paths for generalized linear models via coordinate descent. *J Stat Softw* 33:1–22
28. Dormann CF, Elith J, Bacher S et al (2013) Collinearity: a review of methods to deal with it and a simulation study evaluating their performance. *Ecography* 36(1):27–46
29. Kuhn M (2008) Building Predictive Models in R Using the caret Package. 2008 28:26 %. *J Stat Soft*
30. Park JE, Han K, Sung YS et al (2017) Selection and reporting of statistical methods to assess reliability of a diagnostic test: conformity to recommended methods in a peer-reviewed journal. *Korean J Radiol* 18:888–897
31. Park JE, Park SY, Kim HJ, Kim HS (2019) Reproducibility and generalizability in radiomics modeling: possible strategies in radiologic and statistical perspectives. *Korean J Radiol* 20:1124–1137
32. Xue C, Yuan J, Lo GG et al (2021) Radiomics feature reliability assessed by intraclass correlation coefficient: a systematic review. *Quant Imaging Med Surg* 11:4431–4460
33. Lunardon N, Menardi G, Torelli N (2014) ROSE: a package for binary imbalanced learning. *The R Journal* 6(1):79–89
34. DeLong ER, DeLong DM, Clarke-Pearson DL (1988) Comparing the areas under two or more correlated receiver operating characteristic curves: a nonparametric approach. *Biometrics* 44:837–845
35. Sohn B, Choi YS, Ahn SS et al (2021) Machine learning based radiomic HPV phenotyping of oropharyngeal SCC: a feasibility study using MRI. *Laryngoscope* 131:E851–e856
36. Van Griethuysen JJ, Fedorov A, Parmar C et al (2017) Computational radiomics system to decode the radiographic phenotype. *Cancer research* 77:e104–e107
37. Mayerhoefer ME, Materka A, Langs G et al (2020) Introduction to radiomics. *J Nucl Med* 61:488–495
38. Caudell JJ, Gillison ML, Maghami E et al (2022) NCCN Guidelines[®] insights: head and neck cancers, version 1.2022. *J Natl Compr Canc Netw* 20:224–234
39. Le QT, Fu KK, Kaplan MJ, Terris DJ, Fee WE, Goffinet DR (2000) Lymph node metastasis in maxillary sinus carcinoma. *Int J Radiat Oncol Biol Phys* 46:541–549
40. Kim GE, Chung EJ, Lim JJ et al (1999) Clinical significance of neck node metastasis in squamous cell carcinoma of the maxillary antrum. *Am J Otolaryngol* 20:383–390
41. Sharma A, Tang AL, Takiar V, Wise-Draper TM, Langevin SM (2021) Human papillomavirus and survival of sinonasal squamous cell carcinoma patients: a systematic review and meta-analysis. *Cancers (Basel)* 13(15):3677

Publisher's Note

Springer Nature remains neutral with regard to jurisdictional claims in published maps and institutional affiliations.

Springer Nature or its licensor (e.g. a society or other partner) holds exclusive rights to this article under a publishing agreement with the author(s) or other rightsholder(s); author self-archiving of the accepted manuscript version of this article is solely governed by the terms of such publishing agreement and applicable law.